

Hydrostatic and chemical pressure tuning of CeFeAs_{1-x}P_xO single crystals

K. Mydeen,^{1,*} E. Lengyel,¹ A. Jesche,^{1,2} C. Geibel,¹ and M. Nicklas^{1,†}

¹Max Planck Institute for Chemical Physics of Solids, Nöthnitzer Str. 40, 01187 Dresden, Germany

²The Ames Laboratory, Iowa State University, Ames, Iowa USA

(Received 23 August 2012; published 22 October 2012)

We carried out a combined P substitution and hydrostatic pressure study on CeFeAs_{1-x}P_xO single crystals in order to investigate the peculiar relationship of the local moment magnetism of Ce, the ordering of itinerant Fe moments, and their connection with the occurrence of superconductivity. Our results evidence a close relationship between the weakening of Fe magnetism and the change from antiferromagnetic to ferromagnetic ordering of Ce moments at $p^* = 1.95$ GPa in CeFeAs_{0.78}P_{0.22}O. The absence of superconductivity in CeFeAs_{0.78}P_{0.22}O and the presence of a narrow and strongly pressure sensitive superconducting phase in CeFeAs_{0.70}P_{0.30}O and CeFeAs_{0.65}P_{0.35}O indicate the detrimental effect of the Ce magnetism on superconductivity in P-substituted CeFeAsO.

DOI: [10.1103/PhysRevB.86.134523](https://doi.org/10.1103/PhysRevB.86.134523)

PACS number(s): 74.70.Xa, 74.25.Dw, 74.62.Fj, 75.20.Hr

The discovery of superconductivity in LaFeAsO_{1-x}F_x¹ and the highest T_c 's up to 55 K observed in F-doped SmFeAsO^{2,3} have sparked tremendous interest among the scientific community. In most of the iron-pnictide materials, the application of hydrostatic pressure or chemical substitution (i) introduces superconductivity by suppressing the Fe spin-density wave (SDW) ordering in the nonsuperconducting parent compound⁴⁻⁷ and (ii) induces systematic changes in T_c in pnictide superconductors.⁸⁻¹⁰

The Fe moments in CeFeAsO order in a commensurate SDW at about 145 K, while the local Ce moments order antiferromagnetically below 3.7 K.¹¹ In general, replacement of As by P results in chemical-pressure-induced superconductivity in 1111- and 122-type Fe-pnictides.¹²⁻¹⁶ Here, CeFeAs_{1-x}P_xO is outstanding among the 1111-type iron-pnictide materials based on rare-earth elements: P substitution also suppresses the Fe-SDW ordering, but the rare-earth magnetism of the Ce moments changes from antiferromagnetic (AFM) at low ($x < 0.3$) to ferromagnetic (FM) at higher P concentrations ($x \geq 0.3$).^{17,18} Only recently, zero resistance was observed in CeFeAs_{0.70}P_{0.30}O single crystals close to the crossover from AFM to FM ordering of the Ce moments in an already ferromagnetically ordered sample.¹⁷ The application of modest pressure leads to an increase of T_c in doped LaFeAsO_{1-x}F_x^{8,9} and LaFePO¹⁰ pnictide superconductors. On the other hand, pressure induces a decrease of T_c in F-doped CeFeAsO and an enhancement of T_c in Co-doped CeFeAsO.^{19,20} So far, no superconductivity was found in undoped CeFeAsO under pressures up to 50 GPa.²¹

In this paper, hydrostatic pressure is used to fine-tune the physical properties of CeFeAs_{1-x}P_xO in the pressure region where the type of the Ce ordering changes and superconductivity has been reported. Application of modest pressures ($p \lesssim 3$ GPa) allows us to tune CeFeAs_{0.78}P_{0.22}O through the interesting region. Our investigations evidence a sudden change of the Ce ordering from AFM to FM at about $p^* \approx 1.95$ GPa, where also the $T_N^{\text{Fe}}(p)$ becomes constant on further increasing pressures. However, we found no indication for superconductivity. In CeFeAs_{0.70}P_{0.30}O and CeFeAs_{0.65}P_{0.35}O we observed weak Fe-SDW ordering, FM ordering of Ce moments, and superconductivity at low pressures. External

pressure clearly separates the FM and superconducting (SC) transition temperatures. In the discussion we will contrast the effect of hydrostatic and chemical pressure.

The details on the preparation and characterization of the single-crystalline CeFeAs_{1-x}P_xO samples can be found in Ref. 22. In the following we use the nominal P concentration x , which was found to be in good agreement with the actual composition.¹⁷ Four-probe electrical-resistance measurements in the ab plane were carried out on single crystals with approximate dimensions $500 \times 150 \times 80$ mm³ using an LR700 resistance bridge. Temperatures down to 1.8 K and magnetic fields up to 14 T were achieved in a Quantum Design PPMS. Magnetic field was applied in the ab plane parallel to the electrical current. Pressures up to 2.85 GPa were generated in a double-layer piston-cylinder-type pressure cell using silicon oil as a pressure transmitting medium.²³ The pressure shift of the SC transition of lead served as a pressure gauge. The narrow transition at all pressures confirmed the good hydrostatic conditions inside the pressure cell.

The normalized electrical resistance $R(T)/R_{300\text{K}}$ of CeFeAs_{0.78}P_{0.22}O for various pressures up to 2.33 GPa is depicted in Fig. 1. At ambient pressure, $R(T)$ exhibits a maximum followed by a pronounced drop attributed to the onset of Fe-SDW ordering at $T_N^{\text{Fe}} = 93$ K and a further kink at $T_N^{\text{Ce}} = 3.5$ K due to the AFM ordering of Ce moments, which is in agreement with Ref. 17. Compared with CeFeAsO, 22% P substitution already suppresses T_N^{Fe} by about 50 K. The feature at T_N^{Fe} shifts to lower temperatures on application of hydrostatic pressure up to $p = 1.95$ GPa. On further increasing pressure, $T_N^{\text{Fe}}(p)$ stays almost constant at about 28 K ($1.95 \text{ GPa} < p < 2.33 \text{ GPa}$). It is important to note that the maximum in $R(T)$ becomes sharper and more pronounced on increasing pressure for $p \leq 1.95$ GPa, whereas above 1.95 GPa it broadens and starts to fade away.

In the following, we focus on the pressure dependence of the Ce ordering. $R(T)/R_{15\text{K}}$ for different pressures is shown in Fig. 2(a). Up to 1.89 GPa application of pressure shifts the kink indicating T_N^{Ce} in $R(T)$ to higher temperatures. On further increasing pressure, the feature in $R(T)$ broadens significantly and shifts to lower temperatures, in contrast to the behavior at low pressures. While at high pressures the

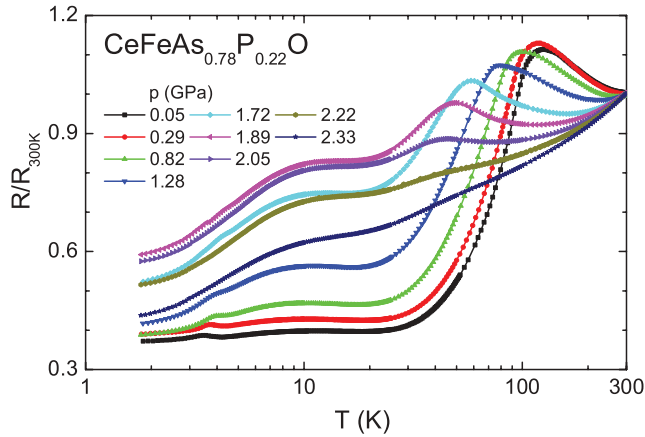


FIG. 1. (Color online) Temperature dependence of the electrical resistance of single-crystalline $\text{CeFeAs}_{0.78}\text{P}_{0.22}\text{O}$ normalized by its value at room temperature under various hydrostatic pressures up to 2.33 GPa.

kink at the transition temperature is hardly visible [we used the maximum in the first derivative of $R(T)$ to determine the transition temperature], the magnetoresistance $\text{MR}_{5T}(T)$ displays a well-defined minimum followed by an increase toward low temperatures due to the Ce ordering [see Fig. 2(b)]. The position of the minimum in $\text{MR}_{5T}(T)$ is in good agreement

with the results from $R(T)$. Initially, $T_N^{\text{Ce}}(p)$ increases with a rate of about 0.5 K/GPa, which is only about half the value reported for polycrystalline CeFeAsO .²¹ We take the abrupt change of the pressure dependence of the ordering temperature and the significantly broadened feature in $R(T)$ above 1.95 GPa as a hint for a change of the Ce ordering at $p^* \approx 1.95$ GPa. Comparing our pressure data with the results of P substitution in $\text{CeFeAs}_{1-x}\text{P}_x\text{O}$ lets us propose that the Ce ordering changes from AFM to FM, which we will substantiate in the following. However, in $\text{CeFeAs}_{0.78}\text{P}_{0.22}\text{O}$ under pressure we observe a decrease in FM Ce ordering temperature (T_C^{Ce}) above 1.95 GPa, in contrast to the increase of T_C^{Ce} observed on chemical pressure by phosphorus substitution. This points to differences between the effect of hydrostatic and chemical pressure on the physical behavior in $\text{CeFeAs}_{1-x}\text{P}_x\text{O}$, which we will address later.

Electrical-resistance measurements in applied magnetic fields give further information on the magnetic ordering of the Ce moments. Figures 2(c)–2(f) depict $R(T)/R_{15\text{K}}$ of $\text{CeFeAs}_{0.78}\text{P}_{0.22}\text{O}$ in different magnetic fields applied parallel to the ab plane for selected pressures. At $p = 0.05$ GPa, a peaklike anomaly in the resistance indicates the AFM ordering of the Ce moments. On increasing magnetic field a more steplike feature develops and shifts to lower temperatures. The monotonous decrease of $T_N^{\text{Ce}}(B)$ is in agreement with the AFM ordering of the Ce moments in the ab plane. At 1.28 GPa only a kink in $R(T)$ remains and marks T_N^{Ce} . However, we still observe the same field dependence of T_N^{Ce} . Also, at 1.72 GPa, we observe a small kink in $R(T)$ shifting to lower temperatures on increasing B . The effect of a small magnetic field $B \leq 0.5$ T on $R(T)$ is tiny until $p^* \approx 1.95$ GPa. In contrast, above p^* a huge effect appears above T_C^{Ce} already at low fields. It is worth mentioning that the value of the change of the resistance in 0.5 T at 2 K is about one order of magnitude larger above p^* than below, substantiating that the Ce magnetism below and above p^* differs fundamentally.

A monotonous decrease of T_N^{Ce} is observed in magnetic fields for $p \leq p^*$ as shown in Fig. 2(g). The $T_N^{\text{Ce}}(B)$ curves for different pressures do not cross; for any fixed magnetic field, $T_N^{\text{Ce}}(p, B)|_{B=\text{const}}$ increases on increasing p . Due to the broadening of the transition anomaly the maximum field up to which we can define T_N^{Ce} decreases with pressure. Figure 2(f) suggests an increase of the ordering temperature with increasing field, but the curves for $B > 0$ do not present a clear kink, allowing for a reliable definition of the transition temperature. This gives a further hint at the change of the Ce ordering from AFM to FM (for $p = 1.89$ GPa no field data is available).

The T - p phase diagram in Fig. 3(a) summarizes the results on $\text{CeFeAs}_{0.78}\text{P}_{0.22}\text{O}$. The transition temperatures deduced from electrical resistance and MR are in good agreement (solid and open symbols, respectively). On application of pressure, T_N^{Ce} decreases monotonously up to $p^* \approx 1.95$ GPa and, on further increasing pressure, T_N^{Ce} is almost constant before its signature in the resistance starts to disappear. $T_N^{\text{Ce}}(p)$ monotonously increases with increasing pressure up to $p^* = 1.95$ GPa. Above p^* our results indicate a sudden change of the type of the Ce ordering from AFM to FM but, in contrast to P substitution in $\text{CeFeAs}_{1-x}\text{P}_x\text{O}$, T_C^{Ce} decreases on further increasing pressure. Up to 2.33 GPa,

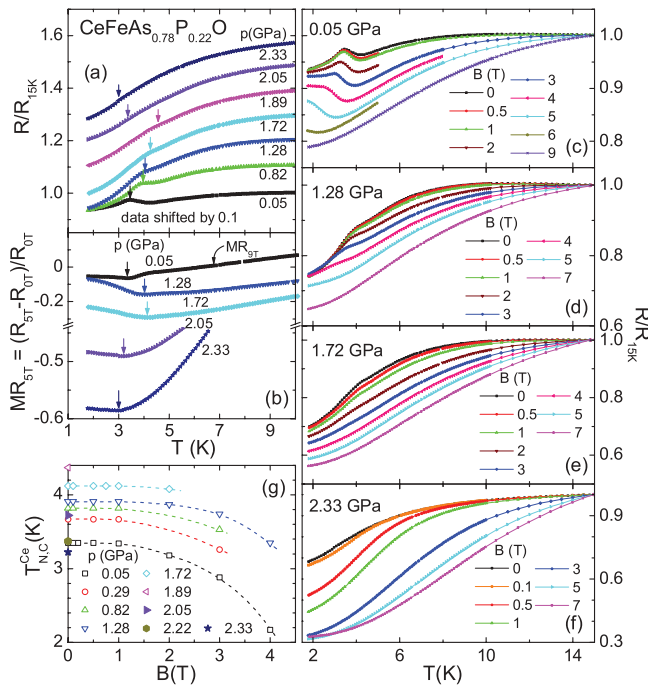


FIG. 2. (Color online) (a) Temperature dependence of $R(T)$ normalized by its value at 15 K of $\text{CeFeAs}_{0.78}\text{P}_{0.22}\text{O}$ for various pressures up to 2.33 GPa (shifted by 0.1). (b) Magnetoresistance with magnetic field applied in the ab plane parallel to the electrical current at different pressures. The arrows in (a) and (b) mark T_N^{Ce} and T_C^{Ce} ; see text for details. [(c)–(f)] Temperature dependence of $R(T)/R_{15\text{K}}$ in different magnetic fields for $p = 0.05$ GPa, 1.28 GPa, 1.72 GPa, and 2.33 GPa. Note the different scales for $R/R_{15\text{K}}$ in (c)–(f). (g) Magnetic field dependence of T_N^{Ce} for various pressures up to 2.33 GPa.

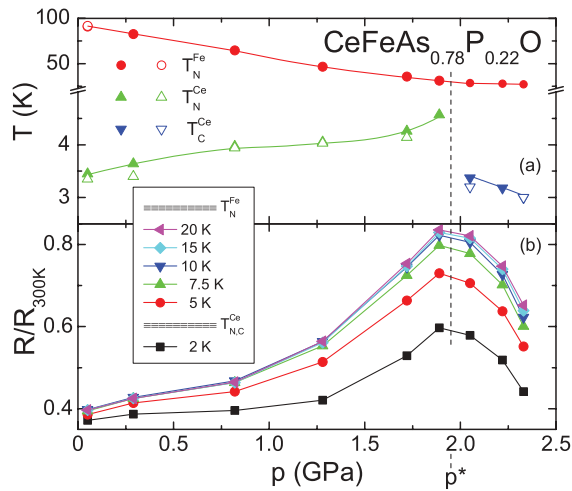


FIG. 3. (Color online) (a) T - p phase diagram of $\text{CeFeAs}_{0.78}\text{P}_{0.22}\text{O}$. Solid and open symbols represent the transition temperatures deduced from $R(T)$ and $\text{MR}(T)$, respectively. (b) Pressure dependence of the isothermal resistance normalized by its value at 300 K.

no indication for superconductivity was found. Even though superconductivity might develop at higher pressure, we note that we found no indication of superconductivity around p^* where the Ce ordering changes from AFM to FM. In this region, superconductivity develops in chemically pressurized $\text{CeFeAs}_{1-x}\text{P}_x\text{O}$.¹⁷

Figure 3(b) displays the normalized isothermal resistance $R_T(p) = R_{T=\text{const}}(p)/R_{300\text{K}}(p)$ at different temperatures. The isothermal resistance at 20 K just below T_N^{Fe} can be considered as a measure of the strength of the Fe moment fluctuations. $R_{20\text{K}}(p)$ possesses a pronounced maximum around 1.95 GPa, where $T_N^{\text{Fe}}(p)$ starts to saturate. Thus, on increasing pressure, the Fe moment fluctuations gradually increase, becoming strongest around 1.95 GPa, and decrease again for higher pressures. On lowering the temperature the maximum stays at the same pressure. Even more surprising, the size of the maximum in $R_T(p)$ remains almost unchanged on reducing temperature from 20 K to 7.5 K, the latter temperature being far below T_N^{Fe} . This indicates that, even at 7.5 K, strong fluctuations of the Fe moments are present. Furthermore, at 5 K and even at 2 K, well below the Ce ordering, a clear maximum shows up in $R_T(p)$. The result at 2 K is remarkable since it evidences the presence of iron moment fluctuations down to the lowest temperatures. We note that at the same pressure where we observe the maximum in $R_T(p)$, the Ce ordering changes from AFM to FM.

We now turn to the samples with higher P content. $\text{CeFeAs}_{0.70}\text{P}_{0.30}\text{O}$ and $\text{CeFeAs}_{0.65}\text{P}_{0.35}\text{O}$ show FM ordering of the Ce moments ($T_C^{\text{Ce}} = 4.1$ K and 4.3 K, respectively) and superconductivity at slightly lower temperatures ($T_c = 3.7$ K and 4.1 K, respectively). In our resistance data we detect only a weak anomaly at the SDW transition at about $T_N^{\text{Fe}} = 38$ K for both concentrations in good agreement with Ref. 17. The results of the pressure experiments for $\text{CeFeAs}_{1-x}\text{P}_x\text{O}$, $x = 0.30$ and 0.35, are similar and summarized in the T - p phase diagram in Fig. 4(a). For both compounds $T_N^{\text{Fe}}(p)$ decreases monotonously on increasing pressure from 38 K

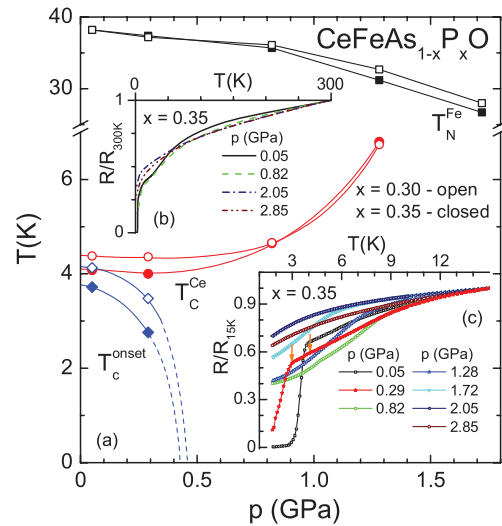


FIG. 4. (Color online) (a) T - p phase diagram for $\text{CeFeAs}_{0.70}\text{P}_{0.30}\text{O}$ and $\text{CeFeAs}_{0.65}\text{P}_{0.35}\text{O}$. (b) $R(T)/R_{300\text{K}}$ for selected pressures. (c) Temperature dependence of the electrical resistance normalized by its value at 15 K for various pressures up to 2.85 GPa. At 0.29 GPa arrows indicate the anomaly at T_C^{Ce} and the onset of the SC transition at T_c^{onset} .

at ambient pressure to below 30 K at 1.72 GPa with an initial rate $d \ln T_N^{\text{Fe}}/dp = -0.084 \text{ GPa}^{-1}$. Above this pressure we can no longer determine T_N^{Fe} from the data.

The observed pressure dependence of T_N^{Fe} is surprising considering the previous results on $\text{CeFeAs}_{0.78}\text{P}_{0.22}\text{O}$. In the comparable pressure regime where the Ce moments order ferromagnetically in $\text{CeFeAs}_{0.78}\text{P}_{0.22}\text{O}$ ($p > 1.95$ GPa), $T_N^{\text{Fe}}(p)$ is almost constant and much smaller than in $\text{CeFeAs}_{0.70}\text{P}_{0.30}\text{O}$ and $\text{CeFeAs}_{0.65}\text{P}_{0.35}\text{O}$ at ambient pressure. This substantiates the different effects of chemical and hydrostatic pressure. At low temperatures, increasing pressure effectively separates $T_c(p)$ and $T_C^{\text{Ce}}(p)$. In $\text{CeFeAs}_{0.65}\text{P}_{0.35}\text{O}$ we find that, on increasing pressure to $p = 0.29$ GPa, $T_c(p)$ decreases from 3.7 K at ambient pressure to 2.7 K, while the feature at $T_C^{\text{Ce}} = 4$ K becomes clearly visible and separated from T_c . Further increasing pressure above 0.29 GPa no longer leaves any signature of superconductivity. However, we were able to detect T_C^{Ce} up to 1.28 GPa before we lose the anomaly in our data. While superconductivity is present, increasing pressure leads to a minute decrease of the ferromagnetic T_C^{Ce} , but once superconductivity disappears, T_C^{Ce} starts to increase significantly with increasing pressure in contrast to the smaller P concentration, $x = 0.22$. For both concentrations, $x = 0.30$ and 0.35, $T_c(p)$ is suppressed to zero temperature at an extrapolated pressure around 0.46 GPa. It is noticeable that the FM Ce ordering cannot be traced in electrical resistance data taken in magnetic fields ($B \geq 0.1$ T) parallel to the ab plane (not shown). This is similar to our findings in $\text{CeFeAs}_{0.78}\text{P}_{0.22}\text{O}$ at pressures above p^* . As expected, the SC transition shifts toward lower temperatures with an increase in the magnetic field. For $x = 0.35$, the upper critical field $\mu_0 H_{c2}^{ab}(0)$ can be estimated to about 1.25 T for 0.05 GPa and only 0.25 T for 0.29 GPa taking $T_c^{\text{onset}}(H)$, indicating that the value of $H_{c2}^{ab}(0)$ is more effectively suppressed by pressure than $T_c(p)$.

In the layered iron pnictides, hydrostatic and chemical pressure reduces the ratio of the c - and a -axis lattice parameters, which results in a strong influence on the antiferromagnetically ordered Fe moment and T_N^{Fe} .²⁴ The chemical pressure by P substitution in $Ln\text{FeAsO}$ ($Ln = \text{Ce, La, Sm}$) compresses the c axis stronger than the a axis and, furthermore, decreases the pnictogen (Pn) height.^{6,7,18,24} The c/a ratio is reduced from 2.151 to 2.142 and the block distance of As-Fe-As from 2.68 Å to 2.58 Å for CeFeAsO and $\text{CeFeAs}_{0.7}\text{P}_{0.3}\text{O}$, respectively. This corresponds to a strong compressing of the FeAs/P layer and, therefore, one expects a strong increase of the hybridization between Fe and Pn states. Accordingly, we observe a strong initial decrease of T_N^{Fe} with hydrostatic pressure by $d \ln T_N^{\text{Fe}}/dp = -0.36 \text{ GPa}^{-1}$ in $\text{CeFeAs}_{0.78}\text{P}_{0.22}\text{O}$ compared with only -0.071 GPa^{-1} in CeFeAsO .²¹ In contrast, chemical pressure results in a stretching of the $Ln\text{O}$ layer,⁶ while hydrostatic pressure results in a compression of this layer.²⁰ This is very likely the reason for the different dependence of T_N^{Ce} and T_C^{Ce} under hydrostatic and chemical pressure. We note that in 122-type Fe-pnictides superconductivity develops on application of hydrostatic pressure and isovalent P substitution on the As site in a quite similar way.¹⁴ This differs from the case of CeFeAsO .

In summary, we carried out a hydrostatic and chemical pressure investigation on $\text{CeFeAs}_{1-x}\text{P}_x\text{O}$ single crystals. In $\text{CeFeAs}_{0.78}\text{P}_{0.22}\text{O}$ we found, first, a fast decrease of $T_N^{\text{Fe}}(p)$ and then, above $p^* = 1.95 \text{ GPa}$, a leveling off at about 28 K. This behavior seems to exclude a quantum critical point scenario in $\text{CeFeAs}_{0.78}\text{P}_{0.22}\text{O}$ under pressure. At p^* the Ce ordering

changes from AFM to FM. Our analysis of the isothermal resistivity suggests the presence of Fe moment fluctuations down to lowest temperatures. We notice that the magnetic ordering of the Ce changes from AFM to FM ordering at the same pressure where we find the maximum in the isothermal resistance. We do not find superconductivity in the region around p^* , in contrast to the results of P substitution in $\text{CeFeAs}_{1-x}\text{P}_x\text{O}$, where superconductivity is observed to co-exist with ferromagnetism close to the P concentration where the AFM Ce ordering changes to FM.¹⁷ The reason could lie in the different responses of $\text{CeFeAs}_{0.78}\text{P}_{0.22}\text{O}$ to pressure and to P substitution, as is evidenced, for example, in the different behavior of $T_{N,C}^{\text{Ce}}$ on pressure and P substitution. However, we point out that we cannot exclude the appearance of superconductivity at pressure higher than our experimentally accessible range. $\text{CeFeAs}_{0.70}\text{P}_{0.30}\text{O}$ and $\text{CeFeAs}_{0.65}\text{P}_{0.35}\text{O}$ are situated right in the narrow P-concentration regime where superconductivity and FM ordering of Ce moments coexist. At ambient pressure we observe a weak Fe-SDW ordering around $T_N^{\text{Fe}} = 38 \text{ K}$ which is suppressed on increasing pressure. In both compounds, increasing pressure enhances $T_C^{\text{Ce}}(p)$. The superconductivity is highly sensitive to pressure and $T_c(p)$ is already suppressed to zero temperature around $p \approx 0.46 \text{ GPa}$. Our study highlights the delicate interplay between iron and cerium magnetism, their sensitivity to structural properties, and, last but not least, the subtle connection to superconductivity.

This work was supported by the DFG within the framework of the SPP1458.

*kamal@cpfs.mpg.de

†nicklas@cpfs.mpg.de

¹Y. Kamihara, T. Watanabe, M. Hirano, and H. Hosono, *J. Am. Chem. Soc.* **130**, 3296 (2008).

²X. H. Chen, T. Wu, G. Wu, R. H. Liu, H. Chen, and D. F. Fang, *Nature* **453**, 761 (2008).

³Z. A. Ren, W. Lu, J. Yang, W. Yi, X. L. Shen, Z. C. Li, G. C. Che, X. L. Dong, L. L. Sun, F. Zhou, and Z. X. Zhao, *Chin. Phys. Lett.* **25**, 2215 (2008).

⁴H. Okada, K. Igawa, H. Takahashi, Y. Kamihara, M. Hirano, H. Hosono, K. Matsubayashi, and Y. Uwatoko, *J. Phys. Soc. Jpn.* **77**, 113712 (2008).

⁵A. S. Sefat, A. Huq, M. A. McGuire, R. Jin, B. C. Sales, D. Mandrus, L. M. D. Cranswick, P. W. Stephens, and K. H. Stone, *Phys. Rev. B* **78**, 104505 (2008).

⁶C. Wang, S. Jiang, Q. Tao, Z. Ren, Y. Li, L. Li, C. Feng, J. Dai, G. Cao, and Z. Xu, *Europhys. Lett.* **86**, 47002 (2009).

⁷N. D. Zhigadlo, S. Katrych, M. Bendele, P. J. W. Moll, M. Tortello, S. Weyeneth, V. Yu. Pomjakushin, J. Kanter, R. Puzniak, Z. Bukowski, H. Keller, R. S. Gonnelli, R. Khasanov, J. Karpinski, and B. Batlogg, *Phys. Rev. B* **84**, 134526 (2011).

⁸H. Takahashi, K. Igawa, K. Arii, Y. Kamihara, M. Hirano, and H. Hosono, *Nature* **453**, 376 (2008).

⁹D. A. Zocco, J. J. Hamlin, R. E. Baumbach, M. B. Maple, M. A. McGuire, A. S. Sefat, B. C. Sales, R. Jin, D. Mandrus, J.

R. Jeffries, S. T. Weir, and Y. K. Vohra, *Physica C* **468**, 2229 (2008).

¹⁰J. J. Hamlin, R. E. Baumbach, D. A. Zocco, T. A. Sayles, and M. B. Maple, *J. Phys.: Condens. Matter* **20**, 365220 (2008).

¹¹A. Jesche, C. Krellner, M. de Souza, M. Lang, and C. Geibel, *New J. Phys.* **11**, 103050 (2009).

¹²C. Wang, L. Li, S. Chi, Z. Zhu, Z. Ren, Y. Li, Y. Wang, X. Lin, Y. Luo, S. Jiang, X. Xu, G. Cao, and Z. Xu, *Europhys. Lett.* **83**, 67006 (2008).

¹³Y. K. Li, X. A. Lin, T. Zhou, J. Q. Shen, Y. K. Luo, Q. A. Tao, G. H. Cao, and Z. Xu, *Physica C* **470**, S493 (2010).

¹⁴S. A. J. Kimber, A. Kreyssig, Y.-Z. Zhang, H. O. Jeschke, R. Valentí, F. Yokaichiya, E. Colombier, J. Yan, T. C. Hansen, T. Chatterji, R. J. McQueeney, P. C. Canfield, A. I. Goldman, and D. N. Argyriou, *Nat. Mater.* **8**, 471 (2009).

¹⁵Z. Ren, Q. Tao, S. Jiang, C. Feng, C. Wang, J. Dai, G. Cao, and Z. Xu, *Phys. Rev. Lett.* **102**, 137002 (2009).

¹⁶H. L. Shi, H. X. Yang, H. F. Tian, J. B. Lu, Z. W. Wang, Y. B. Qin, Y. J. Song, and J. Q. Li, *J. Phys.: Condens. Matter* **22**, 125702 (2009).

¹⁷A. Jesche, T. Förster, J. Spehling, M. Nicklas, M. de Souza, R. Gumeniuk, H. Luetkens, T. Goltz, C. Krellner, M. Lang, J. Sichelschmidt, H.-H. Klauss, and C. Geibel, *Phys. Rev. B* **86**, 020501(R) (2012).

¹⁸Y. Luo, Y. Li, S. Jiang, J. Dai, G. Cao, and Z. A. Xu, *Phys. Rev. B* **81**, 134422 (2010).

- ¹⁹L. Sun, X. Dai, C. Zhang, W. Yi, G. Chen, N. Wang, L. Zheng, Z. Jiang, X. Wei, Y. Huang, J. Yang, Z. Ren, W. Lu, X. Dong, G. Che, Q. Wu, H. Ding, J. Liu, T. Hu, and Z. Zhao, *Europhys. Lett.* **91**, 57008 (2010).
- ²⁰R. S. Kumar, D. Antonio, M. Kanagaraj, S. Arumugam, J. Prakash, S. Sinogeikin, G. S. Thakur, A. K. Ganguli, A. Cornelius, and Y. Zhao, *Appl. Phys. Lett.* **98**, 012511 (2011).
- ²¹D. A. Zocco, R. E. Baumbach, J. J. Hamlin, M. Janoschek, I. K. Lum, M. A. McGuire, A. S. Sefat, B. C. Sales, R. Jin, D. Mandrus, J. R. Jeffries, S. T. Weir, Y. K. Vohra, and M. B. Maple, *Phys. Rev. B* **83**, 094528 (2011).
- ²²A. Jesche, C. Krellner, M. de Souza, M. Lang, and C. Geibel, *Phys. Rev. B* **81**, 134525 (2010).
- ²³S. Klotz, J.-C. Chervin, P. Munsch, and G. Le Marchand, *J. Phys. D* **42**, 075413 (2009).
- ²⁴C. de la Cruz, W. Z. Hu, S. Li, Q. Huang, J. W. Lynn, M. A. Green, G. F. Chen, N. L. Wang, H. A. Mook, Q. Si, and P. Dai, *Phys. Rev. Lett.* **104**, 017204 (2010).